CERN-EP-2022-092  
2022/06/07

CMS-SMP-21-013

# Observation of same-sign $WW$ production from double parton scattering in proton-proton collisions at $\sqrt{s} = 13$ TeV

The CMS Collaboration

## Abstract

The first observation of the production of  $W^+W^\pm$  bosons from double parton scattering processes using same-sign electron-muon and dimuon events in proton-proton collisions is reported. The data sample corresponds to an integrated luminosity of  $138 \text{ fb}^{-1}$  recorded at a center-of-mass energy of 13 TeV using the CMS detector at the CERN LHC. Multivariate discriminants are used to distinguish the signal process from the main backgrounds. A binned maximum likelihood fit is performed to extract the signal cross section. The measured cross section for production of same-sign  $W$  bosons decaying leptonically is  $80.7 \pm 11.2$  (stat) $_{-8.6}^{+9.5}$  (syst)  $\pm 12.1$  (model) fb, whereas the measured fiducial cross section is  $6.28 \pm 0.81$  (stat)  $\pm 0.69$  (syst)  $\pm 0.37$  (model) fb. The observed significance of the signal is 6.2 standard deviations above the background-only hypothesis.

*Submitted to Physical Review Letters*

arXiv:2206.02681v1 [hep-ex] 6 Jun 2022



Double parton scattering (DPS) events, in which two hard parton-parton interactions occur in a single proton-proton (pp) collision have been proposed and studied since the advent of the parton model and hadron colliders [1–9]. The study of such events sheds light on the internal structure of the colliding protons. Primarily, the study of DPS processes provides information on the transverse profile of the proton and its energy evolution, information that is otherwise not accessible in single parton scattering (SPS) events. In addition, processes with two or more hard parton-parton scatterings allow the study of correlations among the partons from the same proton in terms of momentum, flavor, color, and spin.

In the simplest theoretical model [10], the two parton-parton interactions in DPS can be considered entirely uncorrelated, and the expected DPS cross section can be written as the (normalized) product of the SPS cross sections to produce processes A and B independently, as

$$\sigma_{AB}^{\text{DPS}} = \frac{n \sigma_A \sigma_B}{2 \sigma_{\text{eff}}}, \quad (1)$$

where  $n$  is a combinatorial factor that takes a value of unity if  $A = B$ , and two otherwise. The denominator  $\sigma_{\text{eff}}$  can be interpreted as being proportional to the average squared transverse distance between the interacting partons, and it serves as a useful quantity to compare DPS processes in different production modes. Its experimental value ranges between 2–10 (10–25) mb for gluon- (quark-)initiated DPS production processes [11–29]. As the center-of-mass energy of pp collisions increases, so does the density of sea quarks and gluons, which in turn leads to increased DPS contributions to many final states where pairs of heavy particles are produced. These additional DPS contributions can limit the precision of searches for new physics [30] and the accuracy of high-precision standard model analyses [31]. Therefore, it is important to study DPS processes in different production modes and final states. Theoretical advancements [8] have improved upon the simple “geometric” approach on which Eq. (1) is based. The introduction of interparton correlations via double parton distribution functions (dPDF) [32–35], which include parton splitting effects and impact parameter dependence, has led to the first dPDF-based Monte Carlo (MC) event generator for DPS events, dShower [36].

The production of leptonically decaying same-sign (SS)  $W$  boson pairs is a promising process to study DPS [37]. Its experimental signature is rather clean and easy to trigger on, and the SPS  $W^\pm W^\pm$  production is highly suppressed because of two additional partons produced in the final state compared with the opposite-sign configuration. Figure 1 illustrates the production of  $W^\pm W^\pm$  via the DPS and SPS processes at leading order (LO) accuracy in electroweak and perturbative quantum chromodynamics (QCD). The DPS  $W^\pm W^\pm$  production has not been observed experimentally, and the existing searches for the process are not statistically significant due to the size of the available data samples [25, 38].

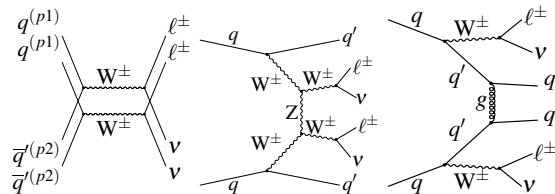


Figure 1: Feynman diagrams for leptonically decaying  $W^\pm W^\pm$  bosons produced via DPS (left) and SPS (middle and right) processes.

This Letter presents the first observation of DPS  $W^\pm W^\pm$  production using pp collision data at  $\sqrt{s} = 13$  TeV. The data sample corresponds to an integrated luminosity of  $138 \text{ fb}^{-1}$  collected using the CMS detector during the 2016–2018 operation of the LHC. The  $W$  bosons are required

to decay into final states consisting of two SS leptons ( $e^\pm\mu^\pm$  or  $\mu^\pm\mu^\pm$ ), including the contributions from leptonic  $\tau$  decays. The dielectron final state is not considered because of the larger background.

The CMS apparatus [39] is a multipurpose, nearly hermetic detector, designed to trigger on [40, 41] and identify electrons, muons, photons, and hadrons [42–45]. A global “particle-flow” (PF) algorithm [46] reconstructs all individual particles in an event, combining information from the silicon tracker, the crystal electromagnetic (ECAL), and the brass-scintillator hadron calorimeters, which all operate within a 3.8 T superconducting solenoid, with data from the gas-ionization muon detectors embedded in the flux-return yoke outside the solenoid.

The reconstructed particles are used to build leptons, jets, hadronically decaying  $\tau$  leptons ( $\tau_h$ ), and missing transverse momentum ( $p_T^{\text{miss}}$ ) [47–49]. The primary vertex (PV) is taken to be the vertex corresponding to the hardest scattering in the event, evaluated using tracking information alone [50]. Jets are reconstructed from charged and neutral PF candidates by the anti- $k_T$  clustering algorithm [51–53] with a distance parameter of 0.4. The  $\tau_h$  candidates are reconstructed via the “hadrons plus strips” algorithm [47]. Events of interest are selected using a two-tiered trigger system. The first level (L1), composed of custom hardware processors, selects events at a rate of around 100 kHz [40]. The second level, known as the high-level trigger, further reduces the event rate to around 1 kHz before data storage [41].

Charged leptons are required to originate from the PV to avoid contributions from additional pp interactions in the same and nearby bunch crossings (pileup). Electrons are identified using a multivariate analysis (MVA) discriminant that combines observables sensitive to the matching of charged-particle tracks in the tracker to the energy deposits in the ECAL and the amount of bremsstrahlung photons emitted along their trajectory [42, 54]. The presence of electrons resulting from asymmetric photon conversions is reduced by requiring their associated track has no missing hits in the innermost layers of the silicon tracker. The identification of muons is based on linking track segments reconstructed in the silicon tracker to hits in the muon detectors [43]. Further selection criteria are applied to ensure the correct assignment of the electric charge of the leptons in the reconstruction [42]. Lepton isolation requirements are imposed following the same approach as in Ref. [55]. The electron (muon) candidates are required to pass minimal kinematic selection criteria of  $p_T > 10 \text{ GeV}$  and  $|\eta| < 2.5$  (2.4) and are referred to as “loose” leptons. Furthermore, electrons falling in the ECAL transition region ( $1.442 < |\eta| < 1.556$ ) are vetoed. The “tight” lepton selection used in the analysis employs an MVA discriminant to separate prompt leptons coming from the decays of W or Z (V) bosons, or  $\tau$  leptons and nonprompt leptons [55]. The nonprompt leptons originate from the decays of light- and heavy-flavor hadrons inside jets produced via strong interactions (QCD multijet), hadrons misidentified as leptons, and electrons from photon conversions. The MVA discriminant is trained using a set of observables related to the lepton kinematics, isolation, and identification, as well as variables relating the lepton to the PV and to the nearest reconstructed PF jet [55]. Reconstructed jets must not overlap with identified electrons, muons, or  $\tau_h$  within  $\Delta R = \sqrt{(\Delta\eta)^2 + (\Delta\phi)^2} < 0.4$ , where  $\phi$  is the azimuthal angle in radians. The DEEPIET b tagging algorithm [56, 57] is used to identify jets originating from the hadronization of b quarks. The chosen working point corresponds to a b-tagging efficiency of 84% and a mistag rate of 11% for light-flavor quark and gluon jets.

Collision events are collected using a combination of single-lepton and dilepton triggers that require the presence of one or two isolated leptons above certain  $p_T$  thresholds [41]. The resulting trigger efficiency is above 98% for events passing the subsequent offline selection criteria.

The dominant background contribution arises from the WZ process, in which both bosons de-

cay leptonically and one of the leptons from the Z boson decay is either out of the detector acceptance or does not pass the lepton identification criteria. The nonprompt-lepton backgrounds include predominantly  $W$ +jets and QCD multijet events, with smaller contributions from  $t\bar{t}$  production. Other sources of background include  $W\gamma^*$  events,  $V\gamma$  events with a photon conversion, and  $ZZ$ , as well as rare backgrounds, which include SPS  $W^\pm W^\pm$ ,  $VVV$ , and  $t\bar{t}V$  production. A minor background contribution stems from Drell–Yan (DY) events when the charge of one lepton is mismeasured. The charge mismeasurement in dimuon events is negligible [43], although it is nonzero for electrons [42]. Hence, the lepton charge misidentification (“charge misid.”) background contributes to the  $e^\pm\mu^\pm$  channel only. The contribution to the signal yield from the production of two overlapping  $W$  bosons from pileup is negligible.

The signal process is characterized by the presence of a pair of SS leptons with a moderate amount of  $p_T^{\text{miss}}$  and little jet activity. The signal region (SR) selection requires events with exactly one pair of  $e^\pm\mu^\pm$  or  $\mu^\pm\mu^\pm$  with  $p_T > 25$  (20) GeV for the leading (subleading) lepton. To reduce the contribution from  $WZ$  background, events having either a third loosely identified lepton with  $p_T > 10$  GeV or a  $\tau_h$  candidate with  $p_T > 20$  GeV and  $|\eta| < 2.3$  are rejected. The contributions from nonprompt-lepton backgrounds are reduced by selecting events with  $p_T^{\text{miss}} > 15$  GeV and dilepton invariant mass,  $m_{\ell\ell} > 12$  GeV.

Events are required to have at most one jet with  $p_T^{\text{jet}} > 30$  GeV within  $|\eta_{\text{jet}}| < 2.4$ . Events with a b-tagged jet having  $p_T^{\text{bjet}} > 25$  GeV and  $|\eta_{\text{bjet}}| < 2.4$  are vetoed to reject top quark events. For the  $e^\pm\mu^\pm$  channel, the dilepton transverse momentum should satisfy  $p_T^{\ell\ell} > 20$  GeV to suppress contributions from  $V\gamma$  and DY processes. To increase the signal sensitivity, events in the SR are split into four lepton flavor and charge categories:  $e^+\mu^+$ ,  $e^-\mu^-$ ,  $\mu^+\mu^+$ , and  $\mu^-\mu^-$ .

The normalization of the  $WZ$  ( $ZZ$ ) background is estimated using  $WZ \rightarrow 3\ell\nu$  ( $ZZ \rightarrow 4\ell$ ) lepton control regions (CR) by means of a maximum likelihood (ML) fit to the invariant mass of the three- (four-)lepton system. The  $WZ \rightarrow 3\ell\nu$  CR is defined by requiring three tight leptons including at least one opposite-sign same-flavor (OSSF) lepton pair with  $|m_{\ell\ell} - m_Z| < 10$  GeV. The invariant mass of the three-lepton system must be  $> 100$  GeV. The leading lepton is required to have  $p_T > 25$  GeV, and trailing leptons with  $p_T > 15$  GeV are selected. The  $p_T^{\text{miss}}$  threshold is raised to 50 GeV for this CR, and the rest of the selection requirements are taken from the SR. The  $ZZ \rightarrow 4\ell$  CR requires an additional fourth tight lepton with  $p_T > 10$  GeV without any requirement on jets and  $p_T^{\text{miss}}$ . Both the OSSF lepton pairs should have  $m_{\ell\ell}$  compatible with the Z boson mass.

Various MC event generators are used to simulate the signal and background processes. The signal process is simulated at LO using the PYTHIA [58], HERWIG [59], and dShower [36] generators. The PYTHIA sample, with leptonically-decaying  $W$  bosons, is taken as the nominal signal sample and it predicts a signal cross section value of  $\sigma_{\text{DPS}}^{W^\pm W^\pm} = 86.4$  fb with the tune CUETP8M1 [14]. The tune dependence of the PYTHIA8 cross section is around 40%, emphasizing the need for an experimental measurement. The sample from HERWIG is used for estimating systematic uncertainties. The PYTHIA v8.226 (8.230) using the NNPDF 2.3 [60] parton distribution functions (PDFs) with the underlying tune CUETP8M1 (CP5 [61]) is used for the simulation of the 2016 (2017 and 2018) data-taking periods. The event generator HERWIG++ (v2.7) [59, 62] using the CTEQ6L1 [63] PDF set with the tune CUETHpps1 [14] is used for the 2016 data-taking period, whereas HERWIG7 (v7.1.4) using the NNPDF 3.1 [64] with PDF set CH3 tune [65] is employed for 2017 and 2018. The dShower generator uses dPDF [33, 66] developed using the LO MSTW2008 [66] PDF set. For a given event generator, neither the underlying event tune nor the PDF sets used to simulate the signal samples impact the kinematic observables relevant to

the analysis.

The WZ background is simulated at next-to-LO (NLO) in QCD with the MADGRAPH5\_aMC@NLO v2.4.2 (2.6.5) generator [67] using the FxFx jet merging scheme [68] for the 2016 (2017 and 2018) data-taking period. The MADGRAPH5\_aMC@NLO generator is also used to simulate  $V\gamma$ ,  $t\bar{t}V$ , and triboson (VVV) production. The POWHEG BOX (v2.0) code [69–71] is used to simulate SPS  $W^\pm W^\pm$ , ZZ, and  $W\gamma^*$  production processes. The simulated samples of backgrounds for the 2016 data-taking period use the NNPDF 3.0 [72, 73] PDF set whereas the NNPDF 3.1 set is used for 2017 and 2018. Background simulations and the dShower event generator are interfaced with PYTHIA8 for modeling of the parton showering, hadronization, and underlying event processes, which have similar versions and tunes as the signal process. The CMS detector response is modeled using GEANT4 [74], and the simulated events are reconstructed with the same algorithms used for the data. Simulated events are weighted to reproduce the pileup distribution measured in the data. The average number of pileup interactions was 23 (32) in 2016 (2017 and 2018). Scale factors are applied to simulated samples to correct for differences in the reconstruction and selection of physics objects and in the trigger efficiencies between simulation and data. These scale factors are measured with the “tag-and-probe” method using DY events [75].

The nonprompt-lepton background is estimated directly from data using the lepton misidentification rate method [55]. The probability for a loose nonprompt lepton to pass the tight lepton selection criteria ( $f_p$ ) is estimated using a data control sample dominated by nonprompt leptons and is parameterized as a function of  $p_T$  and  $|\eta|$ . Events in a sideband of the SR, with at least one lepton failing the tight lepton selection criteria, are reweighted with  $f_p$  to estimate the nonprompt-lepton background contribution. A similar approach is used to estimate the background contribution from “charge misidentification” events by applying the lepton charge misidentification rate to opposite-sign events in data. The charge misidentification rate is about 0.01 (0.10)% for electrons in the barrel (endcap) regions.

Two separate boosted decision tree (BDT) discriminants [76] are trained to distinguish the signal from the WZ and nonprompt-lepton backgrounds. The BDT training against the WZ sample is done using its simulated sample, whereas the training against nonprompt leptons is carried out using a “tight-loose” control sample in data. Kinematic differences between the signal and these backgrounds are explored to define a set of input variables for the training of two discriminants, which are optimized based on their discriminating power. These input variables include: transverse momenta of the two leptons;  $p_T^{\text{miss}}$ ; product and absolute sum of the  $\eta$  of the two leptons; separation in  $\phi$  between the leptons; separation in  $\phi$  between the subleading lepton and  $p_T^{\text{miss}}$ ; separation in  $\phi$  between the dilepton system and the subleading lepton; transverse mass of the two leptons; transverse mass of the leading lepton and  $p_T^{\text{miss}}$ ; and the “stransverse mass” of the dilepton and  $p_T^{\text{miss}}$  system [77, 78]. The two BDT scores are mapped into a two-dimensional (2D) plane in both discriminants. Further, the 2D plane is divided into 13 contiguous regions on which the final fit is performed. This division into regions is performed through optimization of the expected signal significance.

The integrated luminosities for the 2016, 2017, and 2018 data-taking years have individual uncertainties of 1.2–2.5% [79–81], while the overall uncertainty for the 2016–2018 period is 1.6%. The simulation of pileup events assumes an inelastic pp cross section of 69.2 mb, with an associated uncertainty of 5% [82], which impacts the expected signal and background yields by 1%. The uncertainties in data to simulation scale factors corresponding to the lepton trigger, reconstruction, and identification result in an uncertainty of 3.3 (2.8)% for the  $e^\pm\mu^\pm$  ( $\mu^\pm\mu^\pm$ ) final states. This also includes an uncertainty in the scale factors applied to account for the L1 trig-

ger inefficiency observed in the  $|\eta| > 2.0$  region for the 2016 and 2017 data-taking periods [40]. The jet energy scale uncertainties affect the expected event yields by 3%. Uncertainties in the  $p_T^{\text{miss}}$  are calculated by varying the momenta of unclustered particles that are identified neither as a jet nor as a lepton and affect the expected event yields by  $\approx 2\%$ . The uncertainty in the b tagging efficiency has an effect of  $\approx 1.8\%$  on the expected event yields.

For the  $e^\pm\mu^\pm$  ( $\mu^\pm\mu^\pm$ ) channels, a normalization uncertainty of 30 (25)% in the nonprompt-lepton background accounts for the observed variations in the background estimation method when applied to simulated samples. The dependence of  $f_p$  on the kinematics of the event sample in which it is measured is included as a shape uncertainty [55]. A normalization uncertainty of 20% is applied to the “charge misid.” background, covering the differences in the measurement of the charge misidentification rate in data and simulation. The data-to-MC normalization factors of the  $V\gamma$  background, measured using a dedicated CR [83], are close to unity.

A 50% normalization uncertainty is applied to all other small simulated backgrounds, accounting for the theoretical uncertainties in the predicted cross sections. The theoretical uncertainties associated with the choice of the renormalization and factorization scales and the variations in the PDFs and the strong coupling constant [84, 85] affect the simulated background yields by  $\approx 1\%$ . The effect of variation in PDF sets is negligible for the signal simulations. Any residual model dependence of the signal process is estimated by allowing the shape of the final BDT discriminant to vary between the PYTHIA and HERWIG simulations and the resulting effect is small. The statistical uncertainties due to the limited size of the MC samples are treated according to the Barlow–Beeston–lite method [86, 87].

The yield of the DPS  $W^\pm W^\pm$  process in the SR is obtained by performing a binned ML fit simultaneously in the SR and in the two CRs [88–90], i.e., the normalization factors for the WZ and ZZ backgrounds are included as free parameters in the fit together with the signal process. The fit is performed after combining all the background and signal processes in the aforementioned lepton flavor and charge categories, resulting in four independent distributions of the final BDT discriminant per data-taking year. An excess of events with respect to the background-only hypothesis is observed, which is quantified by calculating the p-value using a profile likelihood ratio test statistic [88]. Figure 2 shows the BDT discriminant distribution after the ML fit (post-fit) for the four lepton flavor and sign categories. The contributions from different backgrounds and the signal processes are stacked on top of each other and the associated postfit uncertainties are also shown.

The measured value of  $\sigma_{\text{DPS}}^{W^\pm W^\pm}$  is  $80.7 \pm 11.2$  (stat) $_{-8.6}^{+9.5}$  (syst)  $\pm 12.1$  (model) fb, where the model uncertainty accounts for the difference in cross sections obtained in the acceptance region with the PYTHIA and HERWIG samples. The observed statistical significance of the signal is 6.2 standard deviations above the background-only hypothesis. Separate fits to the  $e^\pm\mu^\pm$  and  $\mu^\pm\mu^\pm$  channels indicate that the two measurements agree within 1.7 standard deviations. The DPS  $W^\pm W^\pm$  production cross section is also measured in a fiducial volume, defined using two generator-level SS “dressed” leptons ( $e^\pm\mu^\pm$  or  $\mu^\pm\mu^\pm$ ) from W boson decays excluding the events with leptonically decaying  $\tau$  leptons. The leptons are dressed by adding the momenta of generator-level photons within a cone of  $\Delta R(\ell, \gamma) < 0.1$  to their momenta, and are required to pass kinematic requirements on the  $p_T$ ,  $\eta$ ,  $m_{\ell\ell}$ , and  $p_T^{\ell\ell}$  variables from the SR selection. The measured fiducial cross section is  $6.28 \pm 0.81$  (stat)  $\pm 0.69$  (syst)  $\pm 0.37$  (model) fb, where the model uncertainty represents the observed difference in fiducial region efficiencies of the PYTHIA and HERWIG samples. The measured values of the inclusive and fiducial cross sections are in agreement with those predicted by PYTHIA8 with tune CUETP8M1 and dShower.

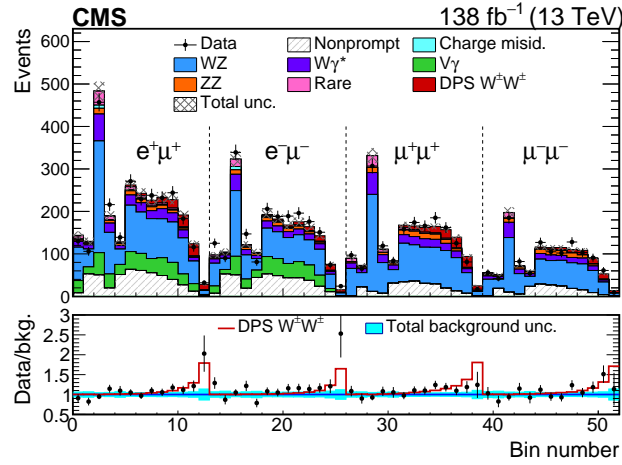


Figure 2: Postfit distribution of the final BDT discriminant output for the four lepton flavor and sign categories. The SPS  $W^\pm W^\pm$ ,  $t\bar{t}V$ , and  $VVV$  contributions are grouped as the “Rare” background. The total postfit uncertainty in the signal and background predictions is shown as the hatched band. The bottom panels show the ratio of data to the sum of all background contributions as the black data points along with the extracted signal shown by the red line. The vertical error bars on the data points represent the statistical uncertainty of the data.

A value of  $\sigma_{\text{eff}}$  is extracted from Eq. (1), using the measured  $\sigma_{\text{DPS}}^{W^\pm W^\pm}$  value and the next-to-NLO prediction for the single  $W^+$  ( $W^-$ ) production cross section including leptonic decays of  $35.4 \pm 1.4$  ( $26.0 \pm 1.0$ ) nb [91, 92]. This procedure results in a value of  $12.2^{+2.9}_{-2.2}$  mb, consistent with previous measurements of this quantity from final states with vector bosons [19, 26]. Tabulated results are provided in HEPData [93].

In summary, the first observation of  $W^\pm W^\pm$  production from double parton scattering processes in proton-proton collisions at  $\sqrt{s} = 13$  TeV has been reported. The analyzed data set corresponds to an integrated luminosity of  $138 \text{ fb}^{-1}$ , collected in 2016–2018 using the CMS detector at the LHC. Events are selected by requiring same-sign electron-muon or dimuon pairs with moderate missing transverse momentum and low jet multiplicity. Boosted decision trees are used to discriminate between the signal and the dominant background processes. A fiducial cross section of  $6.28 \pm 0.81$  (stat)  $\pm 0.69$  (syst)  $\pm 0.37$  (model) fb is extracted, and an inclusive cross section of  $80.7 \pm 11.2$  (stat)  $^{+9.5}_{-8.6}$  (syst)  $\pm 12.1$  (model) fb is measured. This corresponds to an observed significance of the signal above the background-only hypothesis of 6.2 standard deviations. A value of the DPS effective cross section, characterizing the transverse distribution of partons in the proton,  $\sigma_{\text{eff}} = 12.2^{+2.9}_{-2.2}$  mb is extracted.

## References

- [1] N. Paver and D. Treleani, “Multiquark scattering and large- $p_T$  jet production in hadronic collisions”, *Nuovo Cim. A* **70** (1982) 215, doi:10.1007/BF02814035.
- [2] C. Goebel, F. Halzen, and D. M. Scott, “Double Drell-Yan annihilations in hadron collisions: novel tests of the constituent picture”, *Phys. Rev. D* **22** (1980) 2789, doi:10.1103/PhysRevD.22.2789.
- [3] V. P. Shelest, A. M. Snigirev, and G. M. Zinovev, “Gazing into the multiparton distribution equations in QCD”, *Phys. Lett. B* **113** (1982) 325, doi:10.1016/0370-2693(82)90049-1.

- [4] T. Sjöstrand and M. van Zijl, “A multiple interaction model for the event structure in hadron collisions”, *Phys. Rev. D* **36** (1987) 2019, doi:10.1103/PhysRevD.36.2019.
- [5] G. Calucci and D. Treleani, “Disentangling correlations in multiple parton interactions”, *Phys. Rev. D* **83** (2011) 016012, doi:10.1103/PhysRevD.83.016012, arXiv:1009.5881.
- [6] M. Diehl, D. Ostermeier, and A. Schafer, “Elements of a theory for multiparton interactions in QCD”, *JHEP* **03** (2012) 089, doi:10.1007/JHEP03(2012)089, arXiv:1111.0910.
- [7] B. Blok, Yu. Dokshitzer, L. Frankfurt, and M. Strikman, “Perturbative QCD correlations in multi-parton collisions”, *Eur. Phys. J. C* **74** (2014) 2926, doi:10.1140/epjc/s10052-014-2926-z, arXiv:1306.3763.
- [8] M. Diehl and J. R. Gaunt, “Double parton scattering theory overview”, *Adv. Ser. Direct. High Energy Phys.* **29** (2018) 7, doi:10.1142/9789813227767\_0002, arXiv:1710.04408.
- [9] P. Bartalini and J. R. Gaunt, eds., “Multiple parton interactions at the LHC”, volume 29 of *Advanced series on directions in high energy physics*. World Scientific, 2019. doi:10.1142/10646, ISBN 978-981-322-775-0, 978-981-322-777-4.
- [10] J. R. Gaunt, C.-H. Kom, A. Kulesza, and W. J. Stirling, “Same-sign  $W$  pair production as a probe of double parton scattering at the LHC”, *Eur. Phys. J. C* **69** (2010) 53, doi:10.1140/epjc/s10052-010-1362-y, arXiv:1003.3953.
- [11] ATLAS Collaboration, “Measurement of hard double-parton interactions in  $W(\rightarrow l\nu)+2$  jet events at  $\sqrt{s} = 7$  TeV with the ATLAS detector”, *New J. Phys.* **15** (2013) 033038, doi:10.1088/1367-2630/15/3/033038, arXiv:1301.6872.
- [12] CMS Collaboration, “Study of double parton scattering using  $W + 2$ -jet events in proton-proton collisions at  $\sqrt{s} = 7$  TeV”, *JHEP* **03** (2014) 032, doi:10.1007/JHEP03(2014)032, arXiv:1312.5729.
- [13] CDF Collaboration, “Measurement of double parton scattering in  $\bar{p}p$  collisions at  $\sqrt{s} = 1.8$  TeV”, *Phys. Rev. Lett.* **79** (1997) 584, doi:10.1103/PhysRevLett.79.584.
- [14] CMS Collaboration, “Event generator tunes obtained from underlying event and multiparton scattering measurements”, *Eur. Phys. J. C* **76** (2016) 155, doi:10.1140/epjc/s10052-016-3988-x, arXiv:1512.00815.
- [15] D0 Collaboration, “Double parton interactions in  $\gamma + 3$  jet events in  $p\bar{p}$  collisions at  $\sqrt{s} = 1.96$  TeV”, *Phys. Rev. D* **81** (2010) 052012, doi:10.1103/PhysRevD.81.052012, arXiv:0912.5104.
- [16] ATLAS Collaboration, “Observation and measurements of the production of prompt and non-prompt  $J/\psi$  mesons in association with a  $Z$  boson in  $pp$  collisions at  $\sqrt{s} = 8$  TeV with the ATLAS detector”, *Eur. Phys. J. C* **75** (2015) 229, doi:10.1140/epjc/s10052-015-3406-9, arXiv:1412.6428.
- [17] LHCb Collaboration, “Production of associated  $Y$  and open charm hadrons in  $pp$  collisions at  $\sqrt{s} = 7$  and 8 TeV via double parton scattering”, *JHEP* **07** (2016) 052, doi:10.1007/JHEP07(2016)052, arXiv:1510.05949.

- 
- [18] D0 Collaboration, “Evidence for simultaneous production of  $J/\psi$  and  $Y$  mesons”, *Phys. Rev. Lett.* **116** (2016) 082002, doi:10.1103/PhysRevLett.116.082002, arXiv:1511.02428.
- [19] CMS Collaboration, “Observation of triple  $J/\psi$  meson production in proton-proton collisions at  $\sqrt{s} = 13$  TeV”, 2021. arXiv:2111.05370. Submitted to *Nature Physics*.
- [20] AFS Collaboration, “Double parton scattering in pp collisions at  $\sqrt{s} = 63$  GeV”, *Z. Phys. C* **34** (1987) 163, doi:10.1007/BF01566757.
- [21] UA2 Collaboration, “A study of multi-jet events at the CERN  $\bar{p}p$  collider and a search for double parton scattering”, *Phys. Lett. B* **268** (1991) 145, doi:10.1016/0370-2693(91)90937-L.
- [22] CDF Collaboration, “Study of four-jet events and evidence for double parton interactions in  $p\bar{p}$  collisions at  $\sqrt{s} = 1.8$  TeV”, *Phys. Rev. D* **47** (1993) 4857, doi:10.1103/PhysRevD.47.4857.
- [23] CDF Collaboration, “Double parton scattering in  $\bar{p}p$  collisions at  $\sqrt{s} = 1.8$  TeV”, *Phys. Rev. D* **56** (1997) 3811, doi:10.1103/PhysRevD.56.3811.
- [24] LHCb Collaboration, “Observation of double charm production involving open charm in pp collisions at  $\sqrt{s} = 7$  TeV”, *JHEP* **06** (2012) 141, doi:10.1007/JHEP06(2012)141, arXiv:1205.0975. [Addendum: doi:10.1007/JHEP03(2014)108].
- [25] CMS Collaboration, “Constraints on the double-parton scattering cross section from same-sign W boson pair production in proton-proton collisions at  $\sqrt{s} = 8$  TeV”, *JHEP* **02** (2018) 032, doi:10.1007/JHEP02(2018)032, arXiv:1712.02280.
- [26] ATLAS Collaboration, “Study of the hard double-parton scattering contribution to inclusive four-lepton production in pp collisions at  $\sqrt{s} = 8$  TeV with the ATLAS detector”, *Phys. Lett. B* **790** (2019) 595, doi:10.1016/j.physletb.2019.01.062, arXiv:1811.11094.
- [27] CMS Collaboration, “Measurement of double-parton scattering in inclusive production of four jets with low transverse momentum in proton-proton collisions at  $\sqrt{s} = 13$  TeV”, *JHEP* **01** (2022) 177, doi:10.1007/JHEP01(2022)177, arXiv:2109.13822.
- [28] CMS Collaboration, “Study of Z boson plus jets events using variables sensitive to double-parton scattering in pp collisions at 13 TeV”, *JHEP* **10** (2021) 176, doi:10.1007/JHEP10(2021)176, arXiv:2105.14511.
- [29] D0 Collaboration, “Observation and studies of double  $J/\psi$  production at the Tevatron”, *Phys. Rev. D* **90** (2014) 111101, doi:10.1103/PhysRevD.90.111101, arXiv:1406.2380.
- [30] CMS Collaboration, “Search for physics beyond the standard model in events with jets and two same-sign or at least three charged leptons in proton-proton collisions at  $\sqrt{s} = 13$  TeV”, *Eur. Phys. J. C* **80** (2020) 752, doi:10.1140/epjc/s10052-020-8168-3, arXiv:2001.10086.
- [31] A. Del Fabbro and D. Treleani, “A double parton scattering background to Higgs boson production at the LHC”, *Phys. Rev. D* **61** (2000) 077502, doi:10.1103/PhysRevD.61.077502, arXiv:hep-ph/9911358.

- [32] J. R. Gaunt and W. J. Stirling, “Double parton distributions incorporating perturbative QCD evolution and momentum and quark number sum rules”, *JHEP* **03** (2010) 005, doi:10.1007/JHEP03(2010)005, arXiv:0910.4347.
- [33] M. Diehl, J. R. Gaunt, and K. Schönwald, “Double hard scattering without double counting”, *JHEP* **06** (2017) 083, doi:10.1007/JHEP06(2017)083, arXiv:1702.06486.
- [34] M. Diehl, P. Plößl, and A. Schäfer, “Proof of sum rules for double parton distributions in QCD”, *Eur. Phys. J. C* **79** (2019) 253, doi:10.1140/epjc/s10052-019-6777-5, arXiv:1811.00289.
- [35] J. R. Gaunt and T. Kasemets, “Transverse momentum dependence in double parton scattering”, *Adv. High Energy Phys.* **2019** (2019) 3797394, doi:10.1155/2019/3797394, arXiv:1812.09099.
- [36] B. Cabouat, J. R. Gaunt, and K. Ostrolenk, “A Monte Carlo simulation of double parton scattering”, *JHEP* **11** (2019) 061, doi:10.1007/JHEP11(2019)061, arXiv:1906.04669.
- [37] A. Kulesza and W. J. Stirling, “Like sign W boson production at the LHC as a probe of double parton scattering”, *Phys. Lett. B* **475** (2000) 168, doi:10.1016/S0370-2693(99)01512-9, arXiv:hep-ph/9912232.
- [38] CMS Collaboration, “Evidence for WW production from double-parton interactions in proton-proton collisions at  $\sqrt{s} = 13$  TeV”, *Eur. Phys. J. C* **80** (2020) 41, doi:10.1140/epjc/s10052-019-7541-6, arXiv:1909.06265.
- [39] CMS Collaboration, “The CMS experiment at the CERN LHC”, *JINST* **3** (2008) S08004, doi:10.1088/1748-0221/3/08/S08004.
- [40] CMS Collaboration, “Performance of the CMS Level-1 trigger in proton-proton collisions at  $\sqrt{s} = 13$  TeV”, *JINST* **15** (2020) P10017, doi:10.1088/1748-0221/15/10/P10017, arXiv:2006.10165.
- [41] CMS Collaboration, “The CMS trigger system”, *JINST* **12** (2017) P01020, doi:10.1088/1748-0221/12/01/P01020, arXiv:1609.02366.
- [42] CMS Collaboration, “Performance of electron reconstruction and selection with the CMS detector in proton-proton collisions at  $\sqrt{s} = 8$  TeV”, *JINST* **10** (2015) P06005, doi:10.1088/1748-0221/10/06/P06005, arXiv:1502.02701.
- [43] CMS Collaboration, “Performance of the CMS muon detector and muon reconstruction with proton-proton collisions at  $\sqrt{s} = 13$  TeV”, *JINST* **13** (2018) P06015, doi:10.1088/1748-0221/13/06/P06015, arXiv:1804.04528.
- [44] CMS Collaboration, “Performance of photon reconstruction and identification with the CMS detector in proton-proton collisions at  $\sqrt{s} = 8$  TeV”, *JINST* **10** (2015) P08010, doi:10.1088/1748-0221/10/08/P08010, arXiv:1502.02702.
- [45] CMS Collaboration, “Description and performance of track and primary-vertex reconstruction with the CMS tracker”, *JINST* **9** (2014) P10009, doi:10.1088/1748-0221/9/10/P10009, arXiv:1405.6569.

- 
- [46] CMS Collaboration, “Particle-flow reconstruction and global event description with the CMS detector”, *JINST* **12** (2017) P10003, doi:10.1088/1748-0221/12/10/P10003, arXiv:1706.04965.
- [47] CMS Collaboration, “Performance of reconstruction and identification of  $\tau$  leptons decaying to hadrons and  $\nu_\tau$  in pp collisions at  $\sqrt{s} = 13$  TeV”, *JINST* **13** (2018) P10005, doi:10.1088/1748-0221/13/10/P10005, arXiv:1809.02816.
- [48] CMS Collaboration, “Jet energy scale and resolution in the CMS experiment in pp collisions at 8 TeV”, *JINST* **12** (2017) P02014, doi:10.1088/1748-0221/12/02/P02014, arXiv:1607.03663.
- [49] CMS Collaboration, “Performance of missing transverse momentum reconstruction in proton-proton collisions at  $\sqrt{s} = 13$  TeV using the CMS detector”, *JINST* **14** (2019) P07004, doi:10.1088/1748-0221/14/07/P07004, arXiv:1903.06078.
- [50] CMS Collaboration, “Technical proposal for the Phase-II upgrade of the Compact Muon Solenoid”, CMS Technical Proposal CERN-LHCC-2015-010, CMS-TDR-15-02, CERN, 2015.
- [51] M. Cacciari, G. P. Salam, and G. Soyez, “The anti- $k_T$  jet clustering algorithm”, *JHEP* **04** (2008) 063, doi:10.1088/1126-6708/2008/04/063, arXiv:0802.1189.
- [52] M. Cacciari, G. P. Salam, and G. Soyez, “FastJet user manual”, *Eur. Phys. J. C* **72** (2012) 1896, doi:10.1140/epjc/s10052-012-1896-2, arXiv:1111.6097.
- [53] CMS Collaboration, “Pileup mitigation at CMS in 13 TeV data”, *JINST* **15** (2020) P09018, doi:10.1088/1748-0221/15/09/P09018, arXiv:2003.00503.
- [54] CMS Collaboration, “Electron and photon reconstruction and identification with the CMS experiment at the CERN LHC”, *JINST* **16** (2021) P05014, doi:10.1088/1748-0221/16/05/P05014, arXiv:2012.06888.
- [55] CMS Collaboration, “Measurement of the Higgs boson production rate in association with top quarks in final states with electrons, muons, and hadronically decaying tau leptons at  $\sqrt{s} = 13$  TeV”, *Eur. Phys. J. C* **81** (2021) 378, doi:10.1140/epjc/s10052-021-09014-x, arXiv:2011.03652.
- [56] E. Bols et al., “Jet flavour classification using DeepJet”, *JINST* **15** (2020) P12012, doi:10.1088/1748-0221/15/12/P12012, arXiv:2008.10519.
- [57] CMS Collaboration, “Performance of the DeepJet b tagging algorithm using 41.9 fb<sup>-1</sup> of data from proton-proton collisions at 13 TeV with Phase 1 CMS detector”, CMS Detector Performance Note CMS-DP-2018-058, CERN, 2018.
- [58] T. Sjöstrand et al., “An introduction to PYTHIA 8.2”, *Comput. Phys. Commun.* **191** (2015) 159, doi:10.1016/j.cpc.2015.01.024, arXiv:1410.3012.
- [59] M. Bahr et al., “Herwig++ physics and manual”, *Eur. Phys. J. C* **58** (2008) 639, doi:10.1140/epjc/s10052-008-0798-9, arXiv:0803.0883.
- [60] R. D. Ball et al., “Parton distributions with LHC data”, *Nucl. Phys. B* **867** (2013) 244, doi:10.1016/j.nuclphysb.2012.10.003, arXiv:1207.1303.

- [61] CMS Collaboration, “Extraction and validation of a new set of CMS PYTHIA8 tunes from underlying-event measurements”, *Eur. Phys. J. C* **80** (2020) 4, doi:10.1140/epjc/s10052-019-7499-4, arXiv:1903.12179.
- [62] J. Bellm et al., “Herwig 7.0/Herwig++ 3.0 release note”, *Eur. Phys. J. C* **76** (2016) 196, doi:10.1140/epjc/s10052-016-4018-8, arXiv:1512.01178.
- [63] J. Pumplin et al., “New generation of parton distributions with uncertainties from global QCD analysis”, *JHEP* **07** (2002) 012, doi:10.1088/1126-6708/2002/07/012, arXiv:hep-ph/0201195.
- [64] NNPDF Collaboration, “Parton distributions from high-precision collider data”, *Eur. Phys. J. C* **77** (2017) 663, doi:10.1140/epjc/s10052-017-5199-5, arXiv:1706.00428.
- [65] CMS Collaboration, “Development and validation of HERWIG 7 tunes from CMS underlying-event measurements”, *Eur. Phys. J. C* **81** (2021) 312, doi:10.1140/epjc/s10052-021-08949-5, arXiv:2011.03422.
- [66] A. D. Martin, W. J. Stirling, R. S. Thorne, and G. Watt, “Heavy-quark mass dependence in global PDF analyses and 3- and 4-flavour parton distributions”, *Eur. Phys. J. C* **70** (2010) 51, doi:10.1140/epjc/s10052-010-1462-8, arXiv:1007.2624.
- [67] J. Alwall et al., “The automated computation of tree-level and next-to-leading order differential cross sections, and their matching to parton shower simulations”, *JHEP* **07** (2014) 079, doi:10.1007/JHEP07(2014)079, arXiv:1405.0301.
- [68] R. Frederix and S. Frixione, “Merging meets matching in MC@NLO”, *JHEP* **12** (2012) 061, doi:10.1007/JHEP12(2012)061, arXiv:1209.6215.
- [69] P. Nason, “A new method for combining NLO QCD with shower Monte Carlo algorithms”, *JHEP* **11** (2004) 040, doi:10.1088/1126-6708/2004/11/040, arXiv:hep-ph/0409146.
- [70] S. Frixione, P. Nason, and C. Oleari, “Matching NLO QCD computations with parton shower simulations: the POWHEG method”, *JHEP* **11** (2007) 070, doi:10.1088/1126-6708/2007/11/070, arXiv:0709.2092.
- [71] S. Alioli, P. Nason, C. Oleari, and E. Re, “A general framework for implementing NLO calculations in shower Monte Carlo programs: the POWHEG BOX”, *JHEP* **06** (2010) 043, doi:10.1007/JHEP06(2010)043, arXiv:1002.2581.
- [72] NNPDF Collaboration, “Parton distributions with QED corrections”, *Nucl. Phys. B* **877** (2013) 290, doi:10.1016/j.nuclphysb.2013.10.010, arXiv:1308.0598.
- [73] NNPDF Collaboration, “Unbiased global determination of parton distributions and their uncertainties at NNLO and at LO”, *Nucl. Phys. B* **855** (2012) 153, doi:10.1016/j.nuclphysb.2011.09.024, arXiv:1107.2652.
- [74] GEANT4 Collaboration, “GEANT4 — a simulation toolkit”, *Nucl. Instrum. Meth. A* **506** (2003) 250, doi:10.1016/S0168-9002(03)01368-8.
- [75] CMS Collaboration, “Evidence for associated production of a Higgs boson with a top quark pair in final states with electrons, muons, and hadronically decaying  $\tau$  leptons at  $\sqrt{s} = 13$  TeV”, *JHEP* **08** (2018) 066, doi:10.1007/JHEP08(2018)066, arXiv:1803.05485.

- [76] H. Voss, A. Höcker, J. Stelzer, and F. Tegenfeldt, “TMVA, the toolkit for multivariate data analysis with ROOT”, in *XIth International Workshop on Advanced Computing and Analysis Techniques in Physics Research (ACAT)*, p. 40. 2007. arXiv:physics/0703039. [PoS(ACAT)040]. doi:10.22323/1.050.0040.
- [77] C. G. Lester and D. J. Summers, “Measuring masses of semi-invisibly decaying particles pair produced at hadron colliders”, *Phys. Lett. B* **463** (1999) 99, doi:10.1016/S0370-2693(99)00945-4, arXiv:hep-ph/9906349.
- [78] A. Barr, C. Lester, and P. Stephens, “A variable for measuring masses at hadron colliders when missing energy is expected;  $m_{T2}$ : the truth behind the glamour”, *J. Phys. G* **29** (2003) 2343, doi:10.1088/0954-3899/29/10/304, arXiv:hep-ph/0304226.
- [79] CMS Collaboration, “Precision luminosity measurement in proton-proton collisions at  $\sqrt{s} = 13$  TeV in 2015 and 2016 at CMS”, *Eur. Phys. J. C* **81** (2021) 800, doi:10.1140/epjc/s10052-021-09538-2, arXiv:2104.01927.
- [80] CMS Collaboration, “CMS luminosity measurement for the 2017 data-taking period at  $\sqrt{s} = 13$  TeV”, CMS Physics Analysis Summary CMS-PAS-LUM-17-004, CERN, 2018.
- [81] CMS Collaboration, “CMS luminosity measurement for the 2018 data-taking period at  $\sqrt{s} = 13$  TeV”, CMS Physics Analysis Summary CMS-PAS-LUM-18-002, CERN, 2019.
- [82] CMS Collaboration, “Measurement of the inelastic proton-proton cross section at  $\sqrt{s} = 13$  TeV”, *JHEP* **07** (2018) 161, doi:10.1007/JHEP07(2018)161, arXiv:1802.02613.
- [83] CMS Collaboration, “Measurement of the inclusive and differential WZ production cross sections, polarization angles, and triple gauge couplings in pp collisions at  $\sqrt{s} = 13$  TeV”, 2021. arXiv:2110.11231. Submitted to *JHEP*.
- [84] NNPDF Collaboration, “Parton distributions for the LHC Run II”, *JHEP* **04** (2015) 040, doi:10.1007/JHEP04(2015)040, arXiv:1410.8849.
- [85] J. Butterworth et al., “PDF4LHC recommendations for LHC Run II”, *J. Phys. G* **43** (2016) 023001, doi:10.1088/0954-3899/43/2/023001, arXiv:1510.03865.
- [86] R. J. Barlow and C. Beeston, “Fitting using finite Monte Carlo samples”, *Comput. Phys. Commun.* **77** (1993) 219, doi:10.1016/0010-4655(93)90005-W.
- [87] J. S. Conway, “Incorporating nuisance parameters in likelihoods for multisource spectra”, in *PHYSTAT 2011*, p. 115. 2011. arXiv:1103.0354. doi:10.5170/CERN-2011-006.115.
- [88] G. Cowan, K. Cranmer, E. Gross, and O. Vitells, “Asymptotic formulae for likelihood-based tests of new physics”, *Eur. Phys. J. C* **71** (2011) 1554, doi:10.1140/epjc/s10052-011-1554-0, arXiv:1007.1727. [Erratum: doi:10.1140/epjc/s10052-013-2501-z].
- [89] ATLAS and CMS Collaborations, LHC Higgs Combination Group, “Procedure for the LHC Higgs boson search combination in summer 2011”, Technical Report CMS-NOTE-2011-005. ATL-PHYS-PUB-2011-11, CERN, 2011.
- [90] CMS Collaboration, “Precise determination of the mass of the Higgs boson and tests of compatibility of its couplings with the standard model predictions using proton collisions at 7 and 8 TeV”, *Eur. Phys. J. C* **75** (2015) 212, doi:10.1140/epjc/s10052-015-3351-7, arXiv:1412.8662.

- 
- [91] C. Anastasiou, L. J. Dixon, K. Melnikov, and F. Petriello, “High precision QCD at hadron colliders: electroweak gauge boson rapidity distributions at NNLO”, *Phys. Rev. D* **69** (2004) 094008, doi:10.1103/PhysRevD.69.094008, arXiv:hep-ph/0312266.
- [92] R. Gavin, Y. Li, F. Petriello, and S. Quackenbush, “W physics at the LHC with FEWZ 2.1”, *Comput. Phys. Commun.* **184** (2013) 208, doi:10.1016/j.cpc.2012.09.005, arXiv:1201.5896.
- [93] HEPData record for this analysis, 2022. doi:10.17182/hepdata.130562.